Polymorphs by Pressure

M.E. Arroyo y de Dompablo[1], D. Santamaría-Pérez[2] and K. Persson[3]

[1] Dpto. de Química Inorgánica, Universidad Complutense de Madrid, Madrid (Spain)
[2] MALTA Consolider Team, Dpto. de Química Física, Universidad Complutense de Madrid, Madrid (Spain)
[3] Advanced Energy Technology, Lawrence Berkeley National Laboratory, California (US)

1 Thermodynamics of High pressure phase transitions.

There are many interesting and technologically important examples of pressure-induced polymorphism, which is defined as the ability of a solid material to exist in more than one form or crystal structure under different pressures. The most commonly known example may be that of carbon, which transforms at GPa conditions from the malleable graphite structure to the hardest known natural material on Earth – diamond. Figure 1 shows the crystal structure of both allotropes. Let's consider the carbon phase diagram (Figure 2[1]) as typical for a one-component system. The solid lines (co-existence curves) separate the pressure-temperature space into regions where one unique phase is stable. Thus, in Fig 2 we make the general observation that graphite is stable at low pressure, liquid carbon is stable at high temperature and diamond is stable at high pressure.

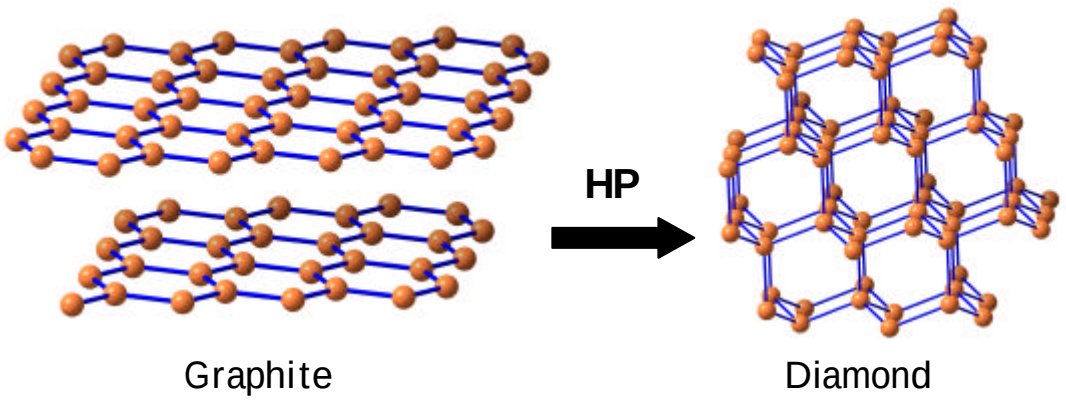

Fig. 1 *Crystal structures of two of the carbon allotropes: graphite and diamond.*

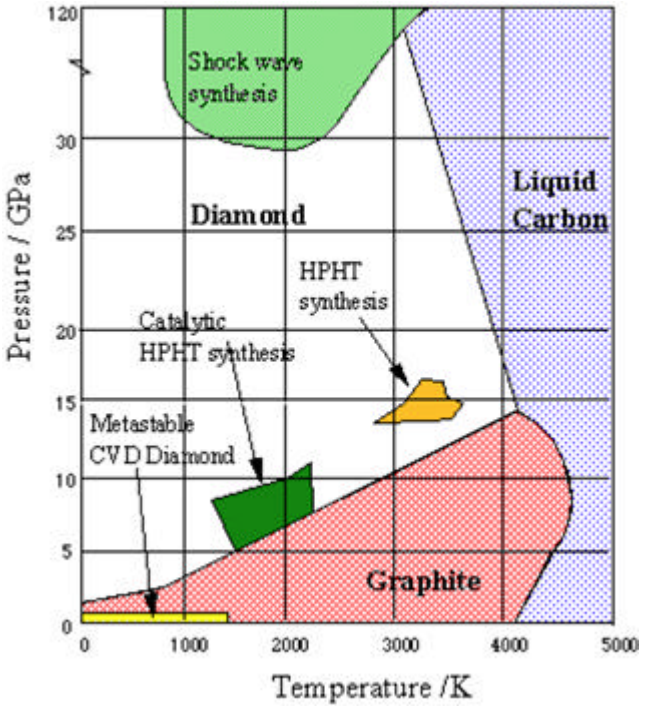

Fig. 2 *Pressure-Temperature phase diagram of carbon as proposed in [1].*

Phase transitions occur as the system passes through one of the coexistence lines and at that point, some thermodynamic properties may go through discontinuities depending on the nature of the transition. Along the coexistence curves the Gibbs free energies for the two phases are equal. Mathematically, Gibbs free energy is described as

$$dG_a = -S_a\,dT + V_a\,dp + E_a \qquad (1)$$

where E is the internal energy, p is the pressure, V is the volume, T is the temperature and S is the entropy of the system. Furthermore, the equality of the Gibbs free energies must hold along any coexistence curve, which means that the following must also be true:

$$dG_a = -S_a\,dT + V_a\,dp + E_a = dG_b = -S_b\,dT + V_b\,dp + E_b \qquad (2)$$

for variations of p and T along the coexistence curve. From this relation we can derive:

$$\left(\frac{dp}{dT}\right)_{transition} = \frac{S_a - S_b}{V_a - V_b} \qquad (3)$$

which is known as the Clausius-Clapeyron equation. It should be stressed that similar equations, expressed in other thermodynamic variables, can be derived for a thermodynamic equilibrium along other coexistence lines**.** For a fixed point on the coexistence line, the temperature is constant and we can conveniently express the slope of the curve at that point in terms of measureable quantities;

$$\left(\frac{dp}{dT}\right)_{\text{fixed T}} = \frac{L_{a\to b}}{T(V_a - V_b)} \qquad (4)$$

where L is called the latent heat and is the heat released/absorbed during a phase transition at constant temperature.

At zero temperature, Gibbs free energy becomes:

$$G = E + pV = H \tag{5}$$

which is denoted the enthalpy *H* of the system. For pressure-induced solid-solid transformations at low temperature, the Gibbs free energy can usually be well approximated with the enthalpy. This means that the stable phase can be found by minimizing the enthalpy. The enthalpy can readily be calculated by first-principles calculations, which makes this method a powerful tool in predicting pressure-induced transitions (for further information, see Sec 2.2).

Both Gibbs free energy and the enthalpy are state functions or state variables, i.e. they are uniquely defined by the state of the system, and not by the way in which the system acquired that state. Other examples of state functions are the entropy *S*, the internal energy *E*, the pressure *p*, the temperature *T* and the volume *V*. Equations of state are useful relations between state variables which describes a system under certain conditions. The most well-known equation of state is probably the ideal gas law which provides a relation between p, V and T for a gas with non-interacting particles. For solids undergoing pressure-induced transition, a useful equation of state is that of the energy as a function of the volume. In this case, the simplest plausible dependence of the two variables is that of a harmonic solid, i.e.

$$E = E_0 + \frac{1}{2} B_0 \frac{(V - V_0)^2}{V_0} \tag{6}$$

where E_0 is the energy for the equilibrium volume V_0 and B_0 is the equilibrium volume bulk modulus of the solid. The bulk modulus is defined as $B = -V\left(\frac{\partial p}{\partial V}\right)_T$ and is related to the compressibility of the solid. A higher bulk modulus signifies a stiffer material. Based on the bulk modulus, we can construct more sophisticated equations of state. One of the most commonly used equations of state is constructed by assuming a constant derivative of the bulk modulus;

$$B' = \left(\frac{\partial B}{\partial p}\right)_T = 0 \tag{7}$$

which when integrated and entered into an expression for the internal energy becomes:

$$E(V) = E_0 + \frac{B_0 V}{B_0'}\left(\frac{(V_0/V)^{B_0'}}{B_0' - 1} + 1\right) - \frac{B_0 V_0}{B_0' - 1} \tag{8}$$

which is called the Murnaghan equation of state [2], where B_0 is the value of B at zero pressure. The Birch-Murnaghan equation of state [3] is a third-order extension of Eq (8). Once equations of state like these are known for a set of polymorphs one can calculate the enthalpies for each phase through $H = E - \left(\frac{\partial E}{\partial V}\right)_S V$ and finally determine the phase with lowest enthalpy, i.e. the stable phase, as a function of pressure.

Pressure-induced phase transformations can be categorized as either displacive or reconstructive. Displacive phase transformations are diffusion-less transitions, which means that they occur between structures that can be transformed into one another by a shear

and/or phonon-related transformation of the lattice. Displacive transitions can occur with or without an activation energy, which is related to the Gibbs free energy landscape around the original structure space.

The Ehrenfest classification scheme for displacive transitions is based on the derivative of the Gibbs free energy around a symmetry point in the parameter space describing the transformation [4, 5]. If there is an activation barrier in the transition path, the first derivative of the Gibbs free energy is discontinuous and the transition is first order (also called martensitic). This, in turn, leads to discontinuities in properties such as the entropy or the volume and release or absorption of energy, called latent heat. Most displacive pressure-induced phase transformations are of first order – an example being the bcc $\rightarrow$ hcp transformation in Fe, which involves both a shear and a phonon mode displacement [6]. If the Gibbs free energy smoothly decreases as a function of the distortion amplitude, there is no activation barrier, and the transformation is second order. Second order transitions are characterized by a continuous development of most system properties.

Several factors influence whether a phase is favoured at high pressure. For example, close-packed phases tend to have smaller equilibrium unit volumes, i.e. smaller Gibbs free energy relative to more open structures. Thus, if one studies phase stability as a function of pressure at zero temperature, one often finds a quite simple evolution from open structures to more close-packed. For some basic examples, see Table 1.

However, within the same chemistry, open structures tend to possess a higher degree of vibrational entropy due to less stiff inter-atomic bonds. Thus, for higher temperatures, open structures generate more entropy, which can stabilize the phase compared to more rigid crystal structures. Well-known examples are the temperature-induced hcp $\rightarrow$ bcc transformations at ~ 1500 K in Ti, Zr and Hf [7]. If one considers both pressure and temperature, there is a competition between volume reduction and entropy production, which means that predicting the stable phase becomes very system-dependent.

Table 1 *Illustrative examples of the difference in equilibrium volumes for low-pressure (LP) and high-pressure (HP) phases in some elements and compounds.*

Compound	Phase	Equilibrium volume ($Å^3$/atom)
Carbon	Graphite (LP) Diamond (HP)	8.8 5.6
Silicon	Cubic diamond (LP) β-tin (HP)	20.0 16.0
Tin	β-tin (LP) bct (HP)	25.3 19.7
AlP	ZnS (LP) NiAs (HP)	39.9 31.9
ZnO	Wurzite (LP) Rocksalt (HP)	11.9 9.7

2 Methods to investigate High-pressure phase transitions

The collaboration between experimentalists and theoreticians is crucial to give new insights into the matter dependence on the two thermodynamic variables (P, T). Materials under extreme conditions are studied with respect to both their chemical and physical properties

(crystal chemistry, melting, equation of state, electronic structure, magnetism, etc…). Several recent reviews on the different HP-HT experimental techniques[8-13], theoretical calculations[14-16] and systematic [14, 17-19] of materials at extreme conditions are available in the literature.

In the last forty years there has been a rapid development of experiments and theory in high-pressure condensed-matter physics. There have also been new progresses in high- and low-temperature experiments which allow us to study the behaviour of the materials over a large P-T range. Thus, nowadays it is possible to produce pressures above 200 GPa ($2 \cdot 10^6$ atmospheres) in static compression experiments, and temperatures that range from a few degrees to more than 5000 K by using cryostats or by focusing laser light onto the sample[8, 10].

Experimental studies are often complemented by theoretical calculations which allow to understand the experimental results and even to predict the behaviour of a given compound at certain conditions. Lattice dynamical calculations can be carried out using either ab initio (first-principles) or empirically derived inter-atomic potentials[15].

2.1 High-pressure experimental techniques

To understand what happens to, for example, the crustal and mantle minerals and the metallic core under P, T conditions inside the Earth, laboratory simulations are usually carried out following one of these two general approaches: (1) Static high pressure or (2) shock compression.

Static high pressure

In this case, the sample is contained in a high-pressure cell. Here, we distinguish between large-anvil cells (LAC) and diamond-anvil cells (DAC). Large-anvil cells are the piston-cylinder apparatus (up to about 8 GPa) and the multianvil presses (up to a few tens of GPa) that compress a few cubic millimetres of sample. Secondary calibrations are often used to measure pressure: Equations of state of simple substances, fluorescence of ruby, etc…These standards has been previously calibrated against a primary standard based on the equation: Pressure = force/area (primary pressure gauge). Monochromatic synchrotron radiation of high brilliance (e.g. Third generation synchrotrons: ESRF, APS or Spring-8) with modern detectors yields in situ information of the crystalline and electronic structure of these small samples. Several characterization techniques as X-ray diffraction (XRD), neutron diffraction (ND), X-ray absorption spectroscopy (XAS) techniques including both Extended X-Ray Absorption Fine Structure (EXAFS) and X-ray Absorption Near Edge Structure (XANES) are used in combination with LAC devices [20].

In diamond-anvil cells (shown in figure 3), a tiny specimen (few microns) is compressed between the tips of two diamonds. Since the surface of the culet size of the diamonds is very small, the force per unit area can reach very high pressures (> 200 GPa). In these studies, the sample can be observed through the diamonds, which may thus serve as a window as well. Many earlier monographs discussed how to operate the DACs and its applications[8, 12]. Besides the characterization techniques mentioned for LAC, in the diamond-anvil cells is also possible to do optical absorption, Raman, Brillouin or Mössbauer spectroscopy measurements[20]. High temperatures can be reached by heating the sample with a high-stable laser. Temperatures are usually measured pirometrically, fitting the Planck equation:

$$I = \frac{e * C_1 * l^{-5}}{(e^{(C_2/(l*T))} - 1)} \qquad (9)$$

to the collected thermal radiation intensity I(λ), where, C_1 and C_2 are constants and ε is the emissivity, which is generally assumed to be independent of wavelength (grey-body approximation) in the visible range.

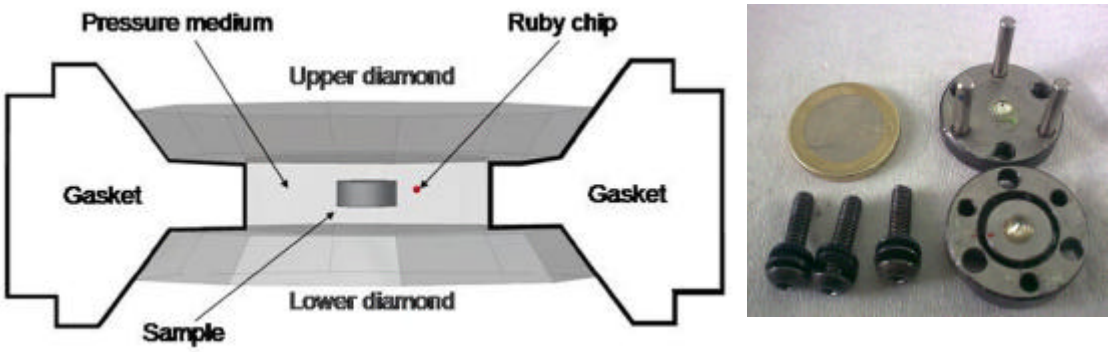

Fig. 3 *Diamond anvil cell*

Shock compression

In this second case, the matter is compressed by shock waves which are usually generated by gas guns. Gas guns produce dynamic pressures by impact of high-velocity projectiles and the passage of shock waves at supersonic speed in the medium. These extreme conditions are applied for only a very short time (about 1 μs) and therefore fast electronic, optical and X-rays characterization techniques are needed[13].

The thermodynamic process at the shock front is assumed to be adiabatic and the temperature rises as a consequence of the compression of the material. Discontinuities in the sound velocity measurements are attributed to phase transitions. The temperatures can be estimated by carefully measuring the radiation emitted by the sample (very complicated measurements), but they are usually calculated on estimates of the specific heat and the Gruneisen parameter.

2.2 Computational Techniques

First principles calculations are highly suitable for predicting pressure-induced phase transformations. Typically, the search for the stable high-pressure phases in a certain chemistry starts out with a 'rounding up of the usual suspects', which means that a reasonably large number of potential crystal structures, restricted by number of atoms in the unit cell and particular space-group symmetries, are calculated for a set of discrete volumes. Figure 4 [21] illustrates the typical output data, in this case for Si, from a series of first-principles total-energy calculations with fixed symmetry. The E(V) data points are then used to fit an E(V) equation of state, from which we can derive the enthalpy, as outlined in Section 1. Minimizing the enthalpy as a function of phase and pressure yields the sequence of stable phases with increased pressure. An equivalent graphical method of finding the transition pressure between two phases is the common tangent construction. In Fig. 4 the β-tin- and the cubic diamond (cd)-type phases of Si have equal enthalpies at the two points $E_{\beta\text{-tin}}(V_1)$ and $E_{cd}(V_2)$ respectively, where a common tangent touches the two energy-volume curves. The negative slope of the tangent gives the equilibrium pressure.

It is important to point out that the equilibrium pressure does not always equal the actual observed transition pressure. In all first order transitions, there is an energy barrier between the two phases, even if their enthalpies are equal, which needs to be overcome by, for example, thermal energy or increased pressure. For example, diamond is thermodynamically stable above 1.7 GPa at 0 K, yet the graphite - diamond transformation does not occur at low temperature due to its very large activation energy, and it requires both high pressure and high temperature (~5-9 GPa and 1200-2800 K) using transition-metal catalysts [22]. An analysis of the barrier can be performed by first principles by calculating the energy landscape around the two phases and mapping out the minimum activation barrier transition path as a function of the distortion parameters. Several examples of such an analysis can be found in Refs [6, 23-25].

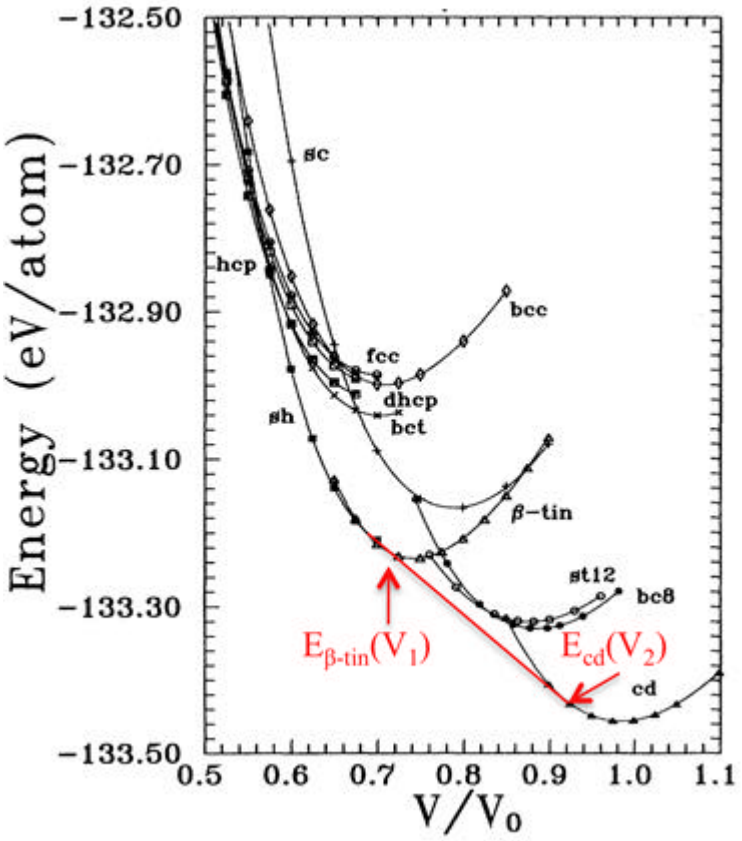

Fig. 4 *The energy (E) vs the volume (V) for 11 phases in Si. The volume is given in terms of the reduced volume, V/V_0exp, where V_0exp = 20.024 A^3/atom is the experimental equilibrium volume of cubic diamond Si. Adapted from [21].*

Most of the calculated phases in Fig 4, for example the 'bc8', 'sc' and 'st12' phases, are higher in enthalpy for all pressures, which means that they are bypassed by the tangent constructions. Such phases are commonly referred to as 'metastable' phases. However, due to kinetic barriers and structural similarities between certain polymorphs these metastable phases can show up, especially under non-equilibrium conditions such as quenching from high temperature. If a system gets 'locked' into a local energy minimum we may observe metastable phases that are not strictly thermodynamically stable.

It is also important to stress that the analysis described above does not include any rigorous consideration of the mechanical stability of the potential high-pressure polymorphs. In calculations the crystal structure is preserved by the symmetry, which means that, in reality, the considered polymorphs may not even represent local energy minima in structure space if the imposed restrictions were relaxed. In principle, all elastic and phonon modes needs to be

examined before a phase can be determined to be truly metastable. These quantities can be obtained from first principles and has been successfully applied to several systems [26-28]. As an illustrative example of the usefulness of such analyses we refer to Ref [26]; as a function of pressure one expects all semiconductor systems show the sequence of ZnS $\rightarrow$ NaCl $\rightarrow$ β-Sn structural phase transitions [29]. This is supported by the common tangent construction, yet experimentally, there is a systematic absence of the NaCl (β-Sn) structure in covalent (ionic) semiconductors. By a complete dynamical analysis of the systems, it is shown that this discrepancy between the predicted sequence of pressure-induced phases and experimental evidence is due to phonon mode instabilities, which do not enter into the simple common tangent construction analysis.

In order to predict high-pressure, high temperature phase transformations we must apply the equilibrium condition to the Gibbs free energy, rather than the enthalpy. At higher temperatures, the entropy difference between different solid phases can become important and needs to be taken into consideration. Entropy contributions are divided into several different categories depending on their physical origin. For example, in many simple elements, the vibrational entropy can play an important role to promote phases with softer bonds. For structural phase transformations involving an accompanying electronic transition, i.e. insulator to metallic, the electronic entropy may influence the sequence of stable phases at higher temperature. The specific entropic contributions can be obtained through tailored statistical mechanics framework analyses, which details are beyond the scope of this book.

3 Systematics on high-pressure phase transitions

Phase stability is governed by pressure and temperature. We saw in section 1 that they have "opposite" effects; increasing pressure favours denser phases, and increasing temperature favours softer phases. Thus, when a solid is subjected to HP/HT conditions there is a competition between volume reduction and entropy production, and the polymorphic transformation that takes place is system-dependent. While no rule of thumb can be established, some systematics can be extracted from a vast number of well known transformations under HP/HT conditions. In this section we focus in general trends of crystal structure and associated chemical bonding/properties evolution of condensed matter under high pressure.

One of the main effects associated with the application of high-pressures to a solid phase is the decrease of the average distances between atoms participating in the involved structures. Such a decrease is correlated with the compressibility of the solid, this is, the bulk modulus, B, introduced in section 1 The electrostatic repulsion between atoms increases, thus causing instability. In order to reduce these adverse effects, the structure changes to another one involving higher coordination numbers of the atoms often associated with larger interatomic distances. Changes in the atomic distances with pressure are countered by the decrease in the volume of the solid, for atom-packing efficiency. Hence, as inferred from table I, high pressure phases show greater density than their low pressure polymorphs.

Several types of structures seem to follow a predetermined route under compression. For example, it is well-known that the compounds with stoichiometry AB follow the sequence NaCl-type $\rightarrow$ CsCl-type. Figure 5 shows these AB structures; pressure induces a densification and an increase of the coordination number around the central atom going from 6 in the NaCl-type to 8 in the CsCl-type. In some systems, intermediate structures might appear, where the central atom is hepta-coordinated, such as the FeB-type or CrB-type. Another example of predetermined route is provided by the compounds AB_2; some compounds such as SiO_2 or GeO_2 undergo transitions under pressure from a rutile-type to a

$CaCl_2$-phase and a α-PbO_2 phase [30]. Although along this sequence of structures the central atom is hexa-coordinated, pressure has a densification effect. Polymorphic transformations of SiO_2 are treated in section 4.6.

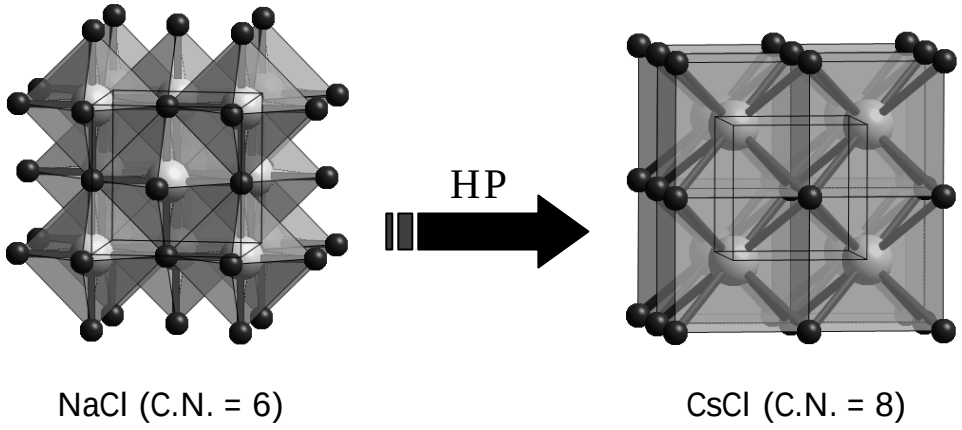

Fig. 5 *Two structural types of AB compounds. In the NaCl-type structure all the atoms are hexa-coordinated whereas in the CsCl-type the coordination number is 8.*

It has also been observed that in several cases the cation subarray of the oxides is the same as that of the structure of the high-pressure phase of the corresponding alloy, without oxygen atoms. On the basis of this fact, an equivalence between oxidation and pressure has been proposed[31]. This interpretation suggests that high-pressure phases of alloys would have structures similar to those of their corresponding oxides (e.g. the alloy BaSn at high pressure adopts a CsCl-type structure, similar to that of the cation subarray (BaSn) in the perovskite $BaSnO_3$).

It is important to remind here the well-known trend that heavier elements, going down a column in the periodic table, adopt the high-pressure structures of their parent lighter elements (e.g. **Na**Cl structure transforms into a **Cs**Cl-type structure at high pressure). However, trends in the crystal behaviour of compounds at high pressure are not well established and represent a complicated challenge for high-pressure scientists. Some interesting examples are also discussed in sections 4.3 and 4.4.

The above transformations of the crystalline structure should be accompanied by modifications in the chemical bonding. A clear illustration is the transition from sp^2 hybridized structure in graphite to the sp^3 hybridized structure of diamond under pressure (see sections 4.4 and 4.5). A general concept is that the increasing in coordination number and lengthening of interatomic distances are associated to an increasing metallic character of the chemical bond. Quite often, polymorphic transformations can be rationalized in terms of electronegative difference concepts. For example, in the MO_2 compound involving highly electropositive transition metals, the transformation under pressure could be driven by electrostatic effects. For example, TiO_2 adopts the 3D rutile structure likely due to the large electronegativity difference between Ti and O (1.54 and 3.44, respectively). On the contrary PtO_2, due to the smaller electronegativity difference between Pt and O (2.28 and 3.44, respectively), can adopt at ambient pressure the layered CdI_2-type structure. Under high pressure conditions – due to the enhancement of the electrostatic repulsion – the a-PtO_2 (CdI_2-type) is transformed to the rutile form (ß-PtO_2) (see [32] and references therein). Another trend is the stabilization of high oxidation states under pressure. Bonding between

transition metals in high formal oxidation states and the surrounding oxygen atoms leads to very short M-O distances, and increasing electrostatic repulsions. Therefore, oxides of transition metal ions in high oxidation states are difficult to prepare at ambient pressure. The influence of a pressure increase is generally the stabilization of a strong covalent bond for unusual oxidation states: compounds with Fe^{4+}, Fe^{5+}, Co^{3+}, Co^{4+}, Ni^{3+}, Cu^{3+}, Ir^{5+}, Ir^{6+} have been prepared under high oxygen pressure ([33] and references therein). A representative example, CrO_2 is further discussed in section 4.9. Six-coordinated high spin iron (IV) has been established in $SrFeO_3$ and $CaFeO_3$ prepared under oxygen pressure [34] [35]). La_2LiFeO_6 prepared under high oxygen pressure has the perovskite structure with the iron in the pentavalent state [36, 37]. Numerous copper oxides related to the High Temperature Superconductors, are also synthesized under medium of high oxygen pressure. $YBa_2Cu_4O_8$ was first prepared under high oxygen pressure [38] (for superconductors see section 4.8).

The intrinsic properties of materials can be drastically altered at high pressures and temperatures (HP-HT), a good example being the superconductivity induced by pressure in LaOFeAs (see section 4.8). Obviously, in a polymorphic transformation, changes in the crystalline structure are coupled to modifications in the electronic structure. Modifications in the electronic structure may occur at the intra-atomic level. As we will see in section 4.9 pressure can induce a change of electronic configuration in transition metal ions from high spin (HS) to low spin (LS). At the inter-atomic scale, the general concept is that pressure induces a “metallization” of the solid. In the simplest picture, for semiconductors the valence and conduction bands broaden under high pressure causing the narrowing of the band gap. Thus, semiconductors tend to transform into a metallic state under compression. This transition takes place in Si at 12 GPa, in Ge at 11 GPa, in Se at 20 GPa in Br at 100 GPa or in Xe at 160 GPa. Even if the metallic state is not reached, generally high pressure polymorphs present improved electronic conductivity compared to their low pressure forms. For instance, in V_2O_5 the calculated density of states shows a narrowing of 0.5 eV in the band gap for the high pressure form, stable above 3 GPa, in comparison to the ambient-pressure material; the measured resistivities at room temperature are 10000 Ωcm and 400 Ωcm for the ambient and high pressure polymorphs, respectively [39]. Similar situation occurs for the polyoxianionic $FePO_4$, with the room temperature resistivity of the high pressure form (2.10^7 Ohm.cm), a form that is stable above 2 GPa, being at least six orders of magnitude smaller than that of the ambient pressure polymorph[40]. However, experimental studies on other semiconductors such as N, show no transition to a metallic state at pressures well above the theoretical prediction, indicating that our understanding of high-pressure transitions in solids is still quite poor. The behaviour of Na under pressure also breaks the “metallization” rule (see section 4.7).

With the materials properties determined by the crystalline and electronic structures, pressure is a valuable variable to produce new materials with interesting properties. In the last 60 years an increasing number of experimental devices and techniques have made possible the synthesis of new materials with outstanding properties important for industrial, technical and scientific applications. Two different strategies become evident: (i) for a given composition high pressure can induce structural transformations, and chemical bonding modifications, leading to new polymorphs not accessible at ambient pressure (ii) treating a mixture of reactants under high pressure/high temperature can create new bonds, leading to the formation of novel materials. In the next section we show the ability of the former to influence the magnetic, electrical and mechanical properties of materials.

4 Condensed Matter under pressure

In this section we will mainly focus on first-order solid-solid phase transitions occurring under high temperature-high pressure conditions. In most cases these transformations have been

observed in X-ray diffraction experiments using a DAC. Measurements at extreme conditions could be performed with almost similar accuracy to ambient conditions, in particular, when the X-ray beam of third generation synchrotrons is used. It is also important to use a quasihydrostatic pressure medium (also non-reactive) to minimize the effects of deviatoric stresses on the sample under study.

The compressibility of the solids is then studied by measuring the lattice constants as a function of pressure (equations of state (EOS) discussed in section 1). In general, we have an increase or decrease of some physical property which depends on the decrease of the distance between atoms. In many cases, we have the appearance of a new crystalline structure at HP-HT conditions. Normally, first-order phase transitions are easily detected by changes in both the position and intensity of the X-ray peaks (different lattice constants and atomic positions, respectively). The phase transition from one solid to another takes place with a change of volume and it is generally accompanied by a sudden change in some physical properties like the electrical conductivity or the sound velocity. In the following sections, a general survey of known high-pressure high-temperature phase transitions that are important in Earth and planetary sciences and material sciences will be given.

4.1 Molecular systems (N_2 and H_2)

The study of diatomic molecular solids, such as H_2, N_2, O_2, etc…, under high pressure is of fundamental interest for condensed matter physics. At low pressures, the atoms forming the molecules are bonded by strong covalent bonds, whereas the molecules interact weakly with each other. At high pressures, both intramolecular and intermolecular interactions become comparable, and ultimately the molecules dissociate. In this section we will focus on two of these molecular systems which exhibit an archetypical behaviour: N_2 and H_2.

The phase diagram of nitrogen is very rich below 50 GPa. At least five solid phases (α, β, γ, δ and ε) have been identified at pressures up to 10 GPa and temperatures below 300 K[41]. At 60 GPa and room temperature, the rhombohedral ε-phase transforms into an orthorhombic ζ-phase[42]. This transition is accompanied by increasing intramolecular and decreasing intermolecular distances. At higher pressures and temperatures, 110 GPa and 2000 K, a major structural transformation takes place in nitrogen. Nitrogen molecules consist of two atoms strongly triple-bonded. However, at the mentioned HP-HT conditions, nitrogen transforms into a polymeric structure (cg-N) with single covalent bonds, similar to carbon atoms in diamond[43]. This crystal structure is shown in figure 6. This new phase is metastable and can not be recovered at room conditions. The cg-N structure represents a new class of energetic materials, with an energy capacity several times higher than that of previous known materials. By the way, this is another example of the fruitful interaction between experimentalists and theoreticians, since this transition was previously predicted by first-principle calculations[44].

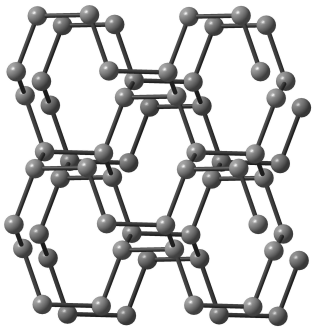

Fig. 6 *Polymeric structure of N (cg-N) formed above 110 GPa.*

The quest for high pressure phases of hydrogen is a long standing one. It was early predicted that hydrogen would suffer an insulator-metal transition at high pressures[45] and, subsequently, Ashcroft suggested that this metallic modification would be a high-temperature superconductor[46]. In the search of this high-pressure phenomenon, three different insulating molecular phases have been clearly observed at room temperature and below[47]. Nowadays, the experimental existence of this metallic phase is still controversial. Nellis et al. observed high electrical conductivity in shock compressed H_2 at 140 GPa and 3000 K[48] and interpreted it as the semiconducting to metallic transition. Diamond cell experiments up to 342 GPa, however, did not find metallic hydrogen in a solid form[49]. It is clear that more studies concerning this subject, both experimental and theoretical, are needed.

4.2 Water

For obvious reasons, the HP-HT phase diagram of water has been a problem of longstanding interest in the fields of chemistry, physics, biology and planetary sciences. Figure 7 shows the water phase diagram. It presents many solid phases (ices): more than twelve crystalline phases and several amorphous ones are reported[50-53]. All the crystalline phases of ice involve the water molecules being hydrogen bonded to four neighbouring water molecules in such a way that a H_2O molecule has two additional hydrogen atoms near each oxygen. These hydrogen bonds are generated by the difference in electronegativity between H and O atoms, which make water molecules polar. When the number of hydrogen bonds per molecule is less than 4, weakness in the ice crystal appears.

However, Pauling predicted that the electrons of the covalent bonds should spread into the hydrogen bonds. At high pressures, this partial covalent character of the hydrogen bonds was observed by infrared spectroscopy using synchrotron radiation[54]. Moreover, Goncharov et al.[55] reported a phase transition on ice at pressures of 60 GPa and temperature below 300K, from a "molecular" system (ice VII) to a dense non-molecular ice (ice X). This new phase is four-times denser than normal ice, is stable up to 210 GPa and their H-O-H bonds are arranged in symmetric way, forming bonds like those of the oxides.

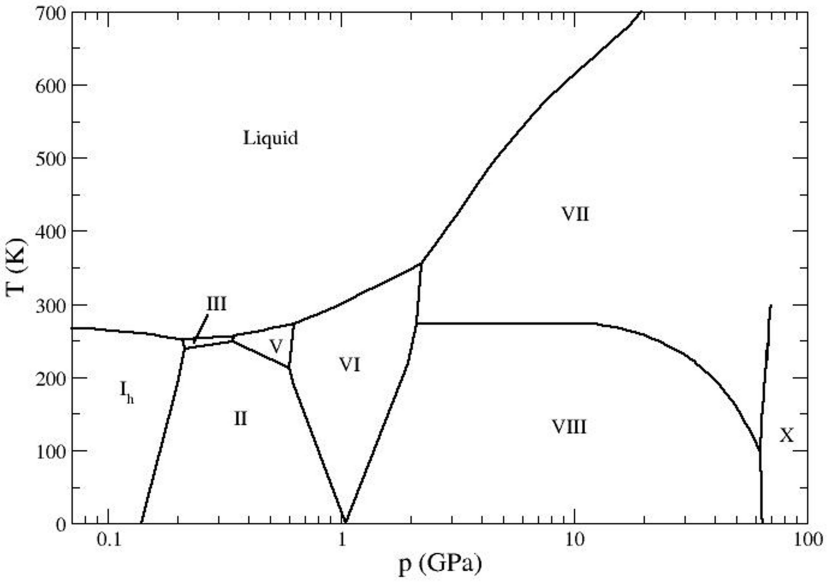

Fig. 7 *Phase diagram of the condensed phases of water. Adapted from [56]*

4.3 Minerals

From seismic data we know that the Earth has a layered structure, which is depicted in figure 8. Experiments at high pressure reveal changes in the mineral structures and properties, and contribute to a better understanding of the different discontinuities. Silicon and oxygen are the Earth most abundant elements and silicate minerals predominate throughout the Earth's crust and mantle. The structure of low-pressure silicates is characterised by the presence of isolated or condensated [SiO_4] tetrahedra. The topology of the tetrahedral linkages provides the basis for the most extended classification of silicates (monosilicates, oligosilicates, ring silicates, chain silicates, layer silicates and tectosilicates). A rich survey of these crystalline structures is the book "Structural Chemistry of Silicates"[57].

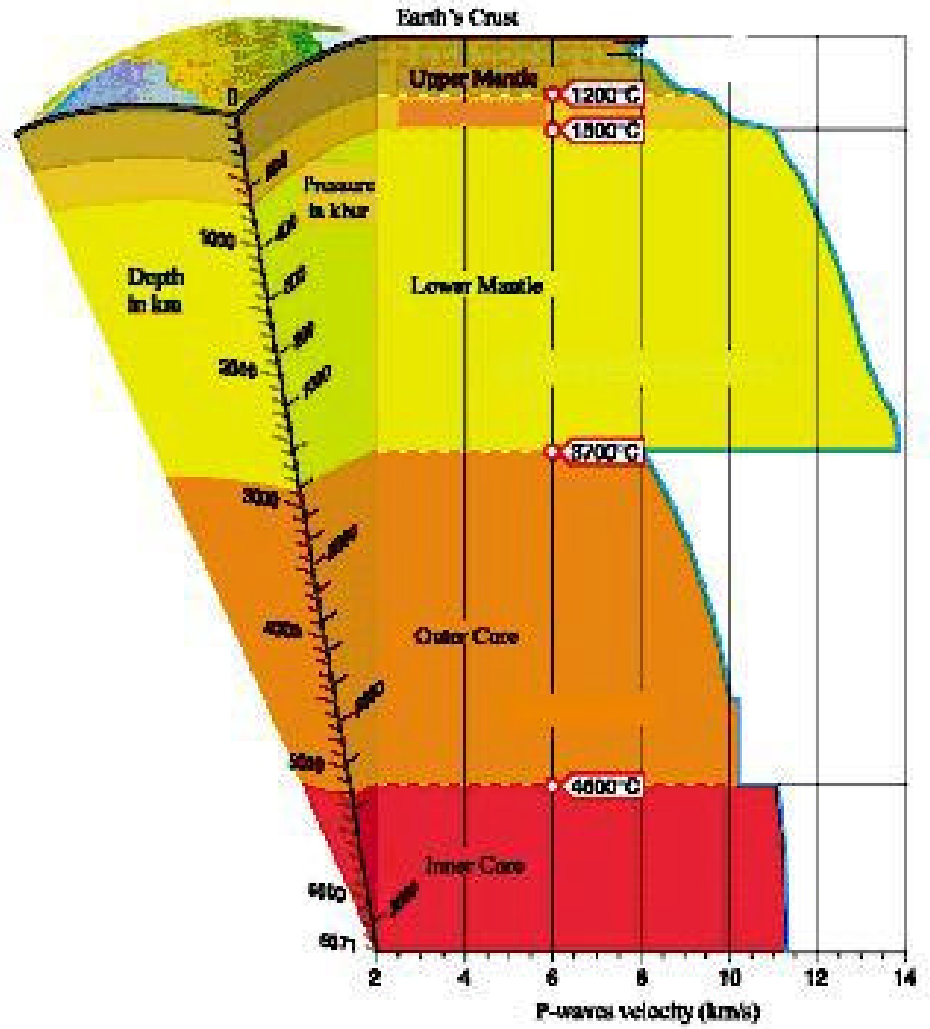

Fig. 8 *Schematic representation of Earth´s interior. The variation with depth of the pressure, temperature and P-waves velocity is shown.*

Several silicates have part or all the silicon atoms hexacoordinated (e.g. garnets, pyrochlores, ilmenites or perovskites). These mineral phases are mainly formed in natural high-pressure environments or quenched from high-pressure experiments. The increase of the coordination number of silicon is usually seen as a consequence of the application of pressure[58]. Some

authors have also reported that the presence of hexacoordinated Si atoms in silicate structures could be the result of the amphoteric behaviour of these atoms[59], i.e. the formation of [SiO_6] octahedra would be related with the electronegativity of the other atoms forming the compound and with the pressure-induced change in its electronic structure.
Perovskite (Mg,Fe)SiO_3 (see figure 9) is assumed to be the dominant mineral structure type in the Earth's lower mantle, accompanied with magnesiowüstite (Mg,Fe)O. This assumption is based in the observed HP-HT phase transition from the pyroxene structure at 23 GPa and 2000 K[60], successfully simulated in a laboratory, and in the properties of the new phase. This phase transition involves the transformation of the tetrahedral coordination of silicon by O atoms in pyroxene into an octahedral coordination in perovskite. The structure and density of perovskite may account for the seismic velocities in the region from 670 to 2700 km in deep[58].

Perovskite and magnesiowüstite are also formed from spinel (Mg,Fe)$_2SiO_4$ at similar conditions (23 GPa and 1600-2100 K), explaining the 670 km discontinuity. This transformation/dissociation has also been reproduced in large volume apparatus experiments[61].

However, it is impossible to explain many of the unusual properties of the lowermost 150 km of the mantle (the D'' layer), assuming only the abovementioned polymorphs. Once again, using HP-HT experiments and *ab initio* simulations, it has recently been shown that, at pressures and temperatures of the D'' layer (i.e. 125 GPa and 2500 K), (Mg,Fe)SiO_3 transforms from perovskite into a layered structure, named post-perovskite (see figure 8)[62, 63]. The elastic properties of the post-perovskite phase and its stability field have explained several observed puzzling properties of the D'' layer, like its seismic anisotropy.

The chemical composition differences and the role of the high pressures and temperatures in the crystal stability is still a vast field for the study of both experimental and theoretical research.

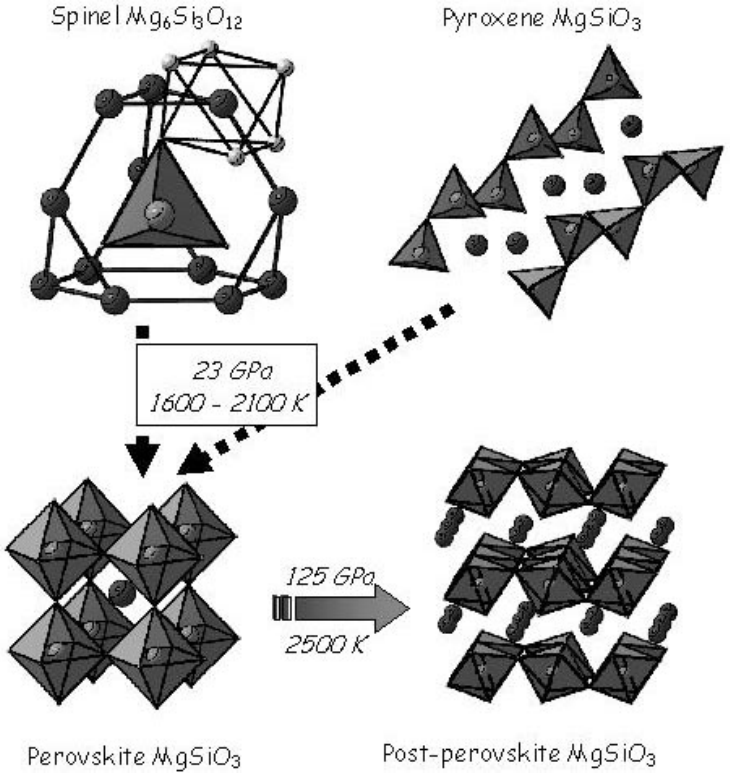

Fig. 9 *Some pressure induced transformations involving (Mg,Fe)SiO_3 in Earth´s interior. The coordination number of the Si atoms increases from 4 to 6 at high pressure (Si atoms in light grey, inside the oxygen polyhedra)*

4.4 Carbon group

Today, most people admire diamonds because of their hardness or/and their brilliance. Nevertheless, diamond is not the most stable allotrope of carbon, which at room conditions adopts the graphite structure (see Figure 1**)**. Natural diamonds are only formed deep inside the Earth's interior where high pressures and high temperatures work together.
Synthetic diamond was first produced in 1953 by the Sweden's electrical company ASEA using a HP-HT apparatus designed by Von Platen[64]. This discovery was kept secret and Bundy et al. of the General Electrics managed to obtain small diamond crystals in a Belt-type apparatus[65]. This group also determined the diamond-graphite equilibrium line[66]: P(GPa) = 0.71 + 2.7E-3·T(K). Nowadays, synthetic diamonds can be formed in much the same way as natural diamonds; graphite is heated to temperatures exceeding 1500ºC at about 6-7 GPa of pressure. This phase transition is currently carried out by big presses and supports a multi-million euro market.

Concerning the emerging of the nano-science, it is important to point out that nanometer-sized diamonds can be obtained at low temperature and low pressure. Thus, a diamond with a grain size below 4 nm is energetically preferred at room conditions compared to nano-graphite, suggesting that the relative stability of both structures is a function of size[67].

The sequence of structures occurring under pressure in the carbon group elements is now well known. Experimental studies up to about 200 GPa have been carried out in diamond-anvil cells[68, 69]. There are some structural homologies between the elements of the carbon group, but they are very limited. The diamond structure occurs in C, Si, Ge and Sn and the β-Sn structure is also adopted in high-pressure phases of Si and Ge. It is a well-known trend that heavier elements, going down a column in the periodic table, adopt the high-pressure structures of their parent lighter elements (i.e. Si adopt the diamond structure of C at room pressure). However, beyond this, there seems to be no other systematic behaviour. The different structures observed could be explained by an increasing role of the d electrons to the structure stability under pressure and, in the case of Pb (the heaviest element of the group), the distinct behaviour can be attributed to relativistic effects. Recent theoretical calculations have proposed displacive mechanisms for all the structural transitions which take place in the elements of group IVa [17].

4.5 Super-hard materials

Hard substances have a high number of strongly directed, covalent chemical bonds per unit volume. They are brittle because the strongly directed bonds favour hardness but not plasticity, which involves the inter-site motion of atoms. At high pressures many brittle materials become ductile. The Mohs scale of mineral hardness characterizes the scratch resistance of various minerals through the ability of a harder material to scratch a softer material. Diamond is the hardest known naturally occurring substance, being at the top of the Mohs scale. The Vickers hardness test is one of the most frequently used to define the hardness of a material [70]. A diamond single-crystal has a Vickers hardness of about 115 GPa. Hard materials rank in the order of 20-40 GPa. Compounds can be defined as super-hard materials, when their micro-hardness exceeds 40 GPa. In addition, super-hard materials possess other unique properties such as compression strength, shear resistance, large bulk moduli, high melting temperatures, chemical inertness, high thermal conductivity, etc., which makes these materials highly desirable for a number of industrial applications.

There is an obvious interest to synthesize new super-hard materials less expensive than diamond. Systems such as B-C-N-O or Si-B-C-N have been extensively explored, with the aim to produce diamond-type materials combining carbon with boron or nitrogen to maintain short and highly covalent bonds. The most common conditions employed to synthesize

super-hard materials involve extreme pressures, or the combination of extreme pressures with temperatures[71]. The super-hardness found in c-BC_2N (Wickers hardness of 76 GPa) [72-74], in the recently reported c-BC_5 (Wickers hardness of 71 GPa) [75] and in c-BN (Wickers hardness of 62 GPa[72]) illustrates the potential of applying high pressure techniques in this field.

Boron nitride presents polymorphic transformations as a function of pressure. At ambient pressure BN possesses the hexagonal structure of graphite (h-BN), at high pressure (5 GPa) h-BN form transforms into a cubic form of the blend (diamond-like) structure, c-BN. Another high-pressure polymorph of h-BN can be produced at 2 GPa, w-BN, with a hexagonal lattice (wurzite-type structure) which can be partially quenched after releasing pressure [76-78]. As in carbon allotropes, the transition from sp^2 hybridized structure in h-BN to sp^3 hybridized structures under pressure induces a dramatic modification in hardness that made c-BN and w-BN second in hardness after diamond for many years.

Recent advances in nanostructure materials lead to the development of super-hard aggregated boron nitride nanocomposites where the decrease of the grain size down to 14 nm and the simultaneous formation of the two dense BN phases with hexagonal and cubic structures within the grains at nano- and subnanolevel result in enormous mechanical property enhancement with maximum hardness of 85(5) GPa [79-81]. Note that the extreme hardness of nanodiamonds prepared under high pressure was reported in the 1990s. This particular diamond material is a series of interconnected nanorods, with diameters of between 5 and 20 nanometres and lengths of around 1 micrometer each[82, 83].

4.6 Dielectrics materials: Piezoelectricity and ferroelectricity

Dielectric properties such as piezoelectricity and ferroelectricity are structure dependent. Piezoelectricity is the ability of some materials (notably crystals and certain ceramics) to generate an electric potential in response to an applied mechanical stress (as pressure). If the material is not short-circuited, the charge separation induces a voltage across the material. The effect is reversible; an applied mechanical stress will generate a voltage, and an applied voltage will change the shape of the solid by a small amount (up to a 4% change in volume). Piezoelectric materials are most widely used as sensors in different environments.

The most well-known piezoelectric material is quartz (SiO_2). Its structure is made up of a continuous framework of [SiO_4] tetrahedra, each oxygen being shared between two tetrahedra (see figure 10). SiO_2 presents a rich polymorphism as a function of temperature and pressure, as represented in figure 11 [84-86]. Tridymite and cristobalite are high-temperature polymorphs of SiO_2 that occur in high-silica volcanic rocks. Coesite is a denser polymorph of quartz found in some meteorite impact sites and in metamorphic rocks formed at pressures greater than those typical of the Earth's crust. Stishovite is a yet denser and higher-pressure polymorph of quartz crystallizing in a rutile-like structure (figure 10). It is found in some meteorite impact sites and is likely to be an important constituent of the Earth's deep mantle. Stishovite is also a prototype for the six-coordinated silicates that are of fundamental importance in geophysics and materials science. With the exception of alpha-cristobalite, and alpha-quartz, the other SiO_2 polymorphs are not piezoeletric.

Other compounds crystallizing in the quartz structure have piezoelectric properties, such as $GaPO_4$ or $AlPO_4$. The high-pressure stability of these piezoelectric materials is of considerable interest, and has been the focus of many investigations (see for instance references [87-96]).

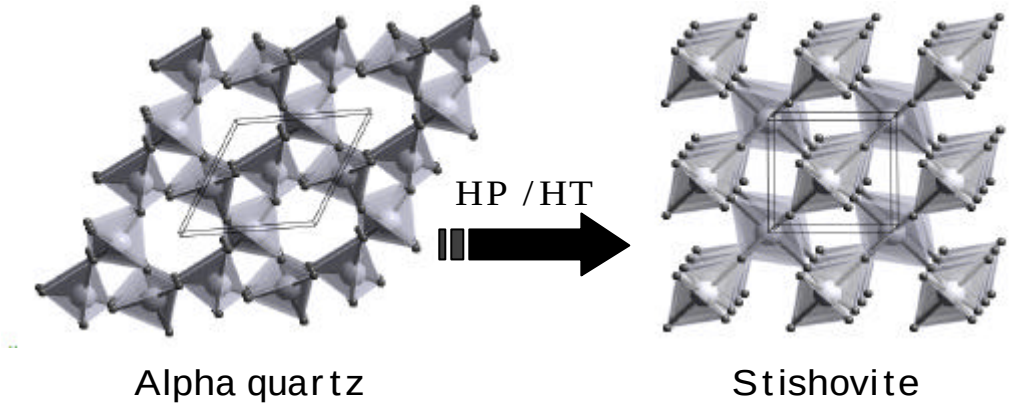

Fig. 10 *The crystal structures of two SiO_2 polymorphs: alpha-quartz and stishovite*

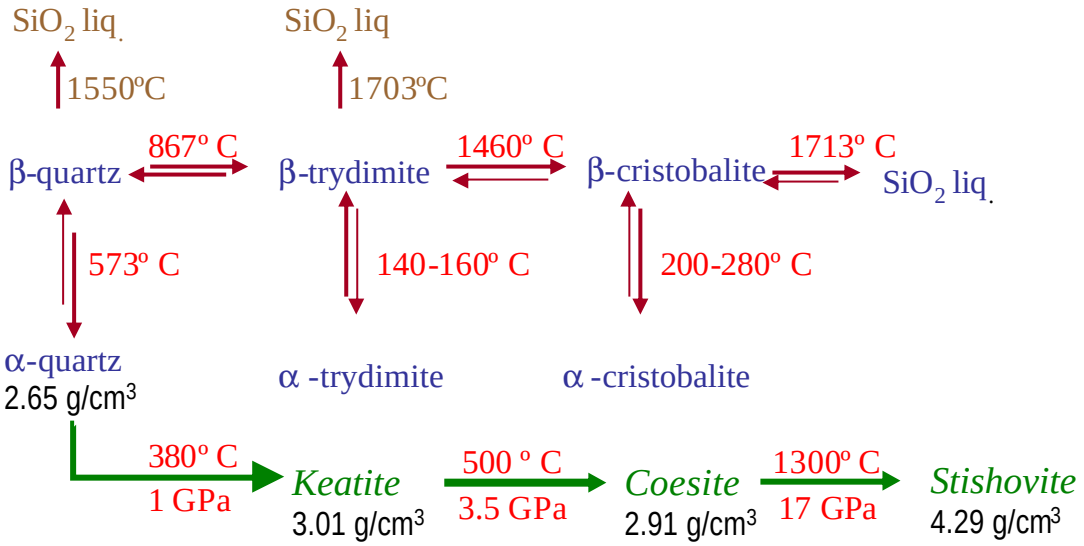

Fig. 11 *Scheme of SiO_2 phase transformation under temperature and pressure. Adapted from references [84-86].*

Ferroelectrics are a type of piezoelectric materials possessing a spontaneous polarization in the absence of an electric field and a mechanical distortion. The direction of the spontaneous electric polarization can be switched (changed) in an applied electric field. Materials only demonstrate ferroelectricity below a certain phase transition temperature, called the Curie temperature, T_c, and are paraelectric above this temperature. The internal electric dipoles of a ferroelectric material are coupled to the material lattice so anything that changes in the lattice will change the strength of the dipoles, this is, the spontaneous polarization. Obviously, the occurrence of ferroelectricity is a matter of the crystal symmetry and a pressure induced transformation may be accompanied by the appearance / disappearance of this property. This is illustrated in the paraelectric compound $[N(CH_3)_4]_2FeCl_4$, which presents several polymorphs as a function of pressure and temperature, some of them being ferroelectrics [97-99]. In particular, a new pressure-induced ferroelectric phase was found at applied pressures between 20 and 70 MPa[99].

Perovskites are an extremely important class of ferroelectric materials. Their importance is not restricted to their technological interest, but also more fundamentally to the understanding of structural phase transitions in solids and related symmetry breaking. Typical examples are $PbTiO_3$ and $BaTiO_3$. Above 393 K $BaTiO_3$ crystallizes in a perfect ABO_3 perovskite structure (shown in figure 8) with cubic symmetry. At 393 K (Tc), a polymorphic transformation to a ferroelectric material with a tetragonal structure occurs. Upon further cooling, it undergoes a

transformation to an orthorhombic structure at 278 K (T1), and to a rhombohedral structure at 183 K (T2). The temperature of these phase transitions is a function of pressure [100-103]. Samara found that Tc and T1 decreases whereas T2 increases as pressure rises, with respective slope -55, -29, and 12.3 K/GPa [101, 102]. Consequently, with increasing pressure, the range of stability of the tetragonal and orthorhombic phase decreases.

4.7 Metals

At ambient pressure, metals are the largest category of elements in the Periodic Table. In general, metals adopt compact and simple high-symmetry crystalline structures, such as bcc (body-centred cubic), fcc (face-centred cubic) or hcp (hexagonal close-packed). It is also well-assumed that at sufficiently high compression all materials must go metallic; as an example we mentioned the metallization of hydrogen in section 4.1. Metals present a too extensive field for this small section, so we will focus on two systems: iron and sodium. For further information on metals at high pressure, see reference [104].

The understanding of the HP-HT phase diagram of iron is very important for several reasons. On one hand, from a technological point of view, iron has interesting physical properties such as magnetism, and its low cost and high strength make it widely used in many engineering applications, commonly in the form of steel. On the other hand, from the geophysical point of view, iron is believed to be the major component of the Earth's core (note two parts in figure 7: solid inner core + liquid outer core). Four phases of iron are stable in the HP-HT diagram (see figure 12) [105-107]: two bcc structures, α and δ, a fcc structure, γ, and an hcp structure, ε. Two extra high-pressure iron phases, an orthorhombic[108] and a dhcp-type[109] (a derivative of the hcp), have been obtained experimentally, probably as a consequence of deviatoric stresses of a hard pressure media. Most of the theoretical and experimental studies suggested that ε-Fe is the only stable phase at high pressures and temperatures. However, there is also a new report of the existence of a bcc-Fe phase above 230 GPa and 3400 K, which could be the stable structure in the Earth's inner core[110].

Contrary to the statement that "all materials must go metallic" at high pressures, sodium does just the opposite. In this case, compression makes core electrons overlap which alters dramatically the electronic properties associated with a free-electron metal[111]. This phenomenon gives rise to the formation of structurally complex phases[112] and the appearance of superconductivity and even insulating states[111].

Researchers found that sodium, a perfect silvery colour metal at room pressure, on increasing pressure first turned black and then, at 200 GPa, red transparent and eventually became a colourless transparent material, like glass. Experimental and computational data identify the new high-pressure phase as a wide band gap dielectric with a distorted double-hexagonal close-packed structure[111]. This result could be relevant for understanding the properties of highly compressed matter.

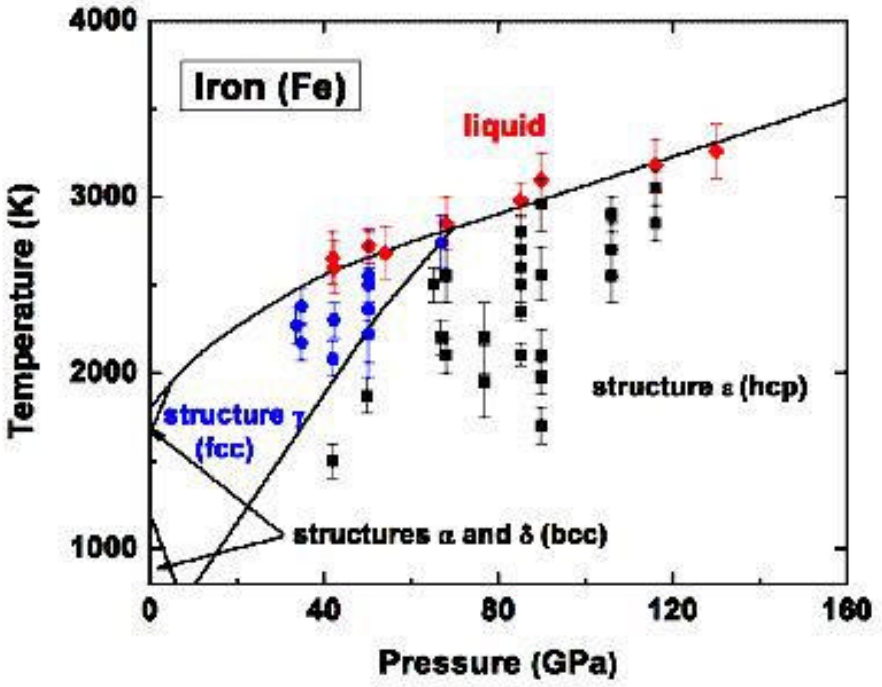

Fig. 12 *Phase diagram of iron according to references [105-107]. X-ray data of the g, e and liquid phases of Fe are represented by blue circles, black squares and red diamonds, respectively.*

4.8 Superconductors

Superconductive materials have the ability to conduct electricity without suffering the effects of electrical resistance, which manifests itself as power loss through heating. This means that a current induced into a circular superconducting wire would theoretically loop around it for an infinite amount of time. The advantages of the use of superconducting materials are obvious when considering the power loss through electrical lines, not to mention that it also enables the use of very powerful magnets to levitate and accelerate trains over their tracks, to travel at high speeds without suffering from friction. To reach the superconducting state, all superconducting materials discovered so far have to be cooled to very low temperatures, below the so-called transition temperature (Tc), which often makes them impractical for widespread use. The early superconductors had to be cooled to extremely low (below 20 K) temperatures. In the 1986, Bednorz and Müller [113] discovered high temperature superconductivity in charge doped cuprate materials, which reach the superconducting state at temperatures of about 135 K. The crystal structure of a typical cuprate HTSC, $HgBa_2Ca_2Cu_3O_8$, is shown in figure 13. Understanding how high temperature superconductors work and thus how they can be manipulated to operate at even higher temperatures, is currently one of the most important unsolved problems in physics.

High-pressure study has played an important role in the investigation of conventional superconductors (Tc < 20 K). Since the discovery of cuprate high temperature superconductors, high-pressure study has become even more important, especially as regards high-pressure synthesis and the effect of pressure. Numerous compounds related to the cuprates superconductors are synthesized subjecting a mixture of reactants to high pressure/high temperature conditions [114-118]. Beyond its involvement in the synthesis process, pressure has an effect on the superconducting properties. Often the Tc of a superconductor can be coaxed upward with the application of high pressure. The superconducting transition temperatures of optimally doped $HgBa_2Ca_{m-1}Cu_mO_{2m+2+d}$ with m=1, 2, and 3 were investigated resistively under quasihydrostatic pressures up to 45 GPa. An

upward shift of Tc under pressure, was found, with a record high Tc of 164 K reached in Hg 1:2:2:3 at 31 GPa [119], which is the highest Tc ever reported. Progresses in experimental settings are critical to further investigate the underlying physics of High Temperature superconductors. Recent technical advances have made possible to investigate the effect of high pressure on cuprates ($Bi_{1.98}Sr_{2.06}Y_{0.68}Cu_2O_{8+\delta}$) using a diamond anvil cell to squeeze the sample and specialized techniques, Raman spectroscopy and X-ray diffraction, to measure the changes in mobile charge carriers, lattice, and magnetism [120].

The discovery of a second family of high Tc materials, the iron-based oxypnictide RFePnO (R= rear earth, Pn = P, As), has led to a resurgence of interest in superconductivity [121-129]. Their crystal structure is composed of alternant stacked Fe-P/As and R-O layers (see figure 13). The charge carrier move in the two-dimensional Fe-P/As layers and the R-O ones play a similar role to that of the insulating block layer in high-Tc cuprates. Unlike the insulating cuprate parent compounds, even the undoped iron oxypnictides are metallic, and superconductivity can be induced by either doping or pressure. Interest in their superconducting properties began in 2006 with the discovery of superconductivity in LaFePO at 4 K [128] and gained much greater attention in 2008 after a large increase in the midpoint Tc of up to 26 K was realized in the isocrystalline compound LaFeAsO on doping of fluoride ions at the O2-sites ($LaO_{1-x}F_xFeAs$) [129]. Increasing the pressure causes a steep increase in the onset Tc of F-doped LaOFeAs, to a maximum of 43 K at 4 GPa.[127]. A high pressure investigation in the related $BaFe_2As_2$ [130] shows that the structural effect of pressure closely mirrors the structural effect of chemical doping. This implies that only structural changes to the parent phase, and not charge doping, are important in inducing superconductivity. Thus, in addition to chemical manipulation, the superconducting state in the iron arsenides can be induced by high pressure. The discovery opens a new window on understanding and harnessing these exciting materials.

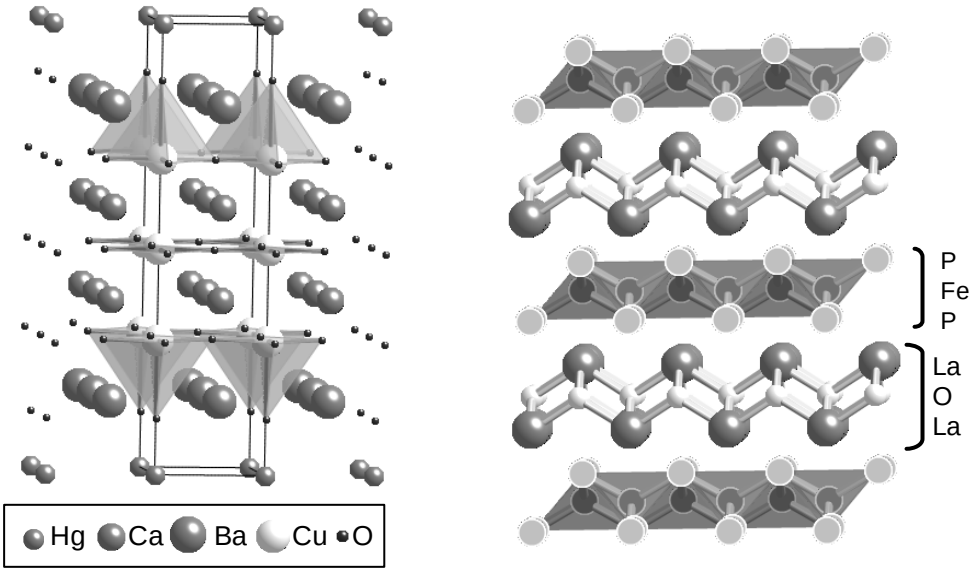

Fig. 13 *Crystal structures of $HgCa_2Ba_2Cu_3O_8$ (left) and LaFePO (right).*

The dependence of superconductivity with pressure has also been investigated in organic superconductors [131-133]. Superconductivity induced by high pressure has been found recently in layered organic Mott insulators [134-136]. ß'-$(BEDT\text{-}TTF)_2ICl_2$. is metallized by application of high pressure up to 9.0 GPa. When the metallic state is stabilized, superconductivity with the highest transition-temperature (Tc) among organic systems appears[135]. The maximum Tc observed was 14.2K at 8.2GPa.

Structural transformation driven by pressure could also produce new superconducting materials. For instance, theoretical work by Babaev and co-workers predicted that in the presence of a magnetic field, liquid metallic hydrogen will exhibit several phase transitions to ordered states, forming two new and unusual quantum states, namely, the metallic superfluid and the superconducting superfluid [137, 138].

4.9 Magnetic materials

Pressure also affects the magnetic properties of materials. A good example is provided by the change in the magnetic properties of FeO. Periclase MgO, wustite FeO, and their solid solutions are of fundamental importance in geoscience because magnesiowustite, (Mg,Fe)O is believed to be one of the main components of Earth´s lower mantle, the second most abundant after the perovskite $(Mg,Fe)SiO_3$. Both oxides are stable in the rocksalt structure (see figure 5), consisting of edge-sharing $[(Fe,Mg)O_6]$ octahedra. The cubic structure of FeO transforms into a rhombohedral structure below 200 K and the material becomes antiferromagnetic. The same transition can be induced by high pressure treatment at ambient temperature [139-141].

FeO has a rich and complex behaviour under high pressure / high temperature, exhibiting a structural phase transition as well as an insulator-metal transition and a spin collapse. Spin collapse, or spin crossover, is a magnetic transition from a high-spin (HS) state to a low-spin (LS) state. The electronic configuration of Fe^{2+} is [Ar] $3d^6$ and, in an octahedral coordination, the *d* levels consist of two sets of orbitals, t^2_g and e_g, which are split according with the octahedral ligand field 10 Dq. In the HS state, the electrons occupy the orbital according to Hunds rule, $(t_{2g})^4$ $(e_g)^2$. In the LS state, the electronic configuration becomes $(t_{2g})^6$ and the total 3*d* magnetic moment is zero. Pressure favours the LS state of transition metal ions, although the actual transition pressure depends on the composition and structure of the material. The magnetic collapse in transition metal oxides MO, crystallizing in the rock-salt type structure, is predicted from first-principles computations at the DFT level at pressures reached in the Earth's lower mantle and core: 149 GPa, 200 GPa , 88 GPa and 230 GPa for M = Mn, Co, Fe and Ni respectively [142]. However, results from the DFT + U calculations suggest that the high-spin magnetic state in FeO should persist to pressures greater than 300 GPa [143]. More recently, DFT+U calculations of the spin transition pressure in rock-salt type $(Mg_{1-x},Fe_x)O$ were performed as a function of composition [144]. It was found that the spin transition pressure decreases with increasing Mg content, consistent with experimental results (see figure 14). According to this computational investigation, the spin transition is primarily driven by the volume difference between the HS and LS phases, rather than changes in the electronic structure with pressure. The magnetic collapse in these structures might have important implications. Seismic anomalies in the outer core and the lowermost mantle may be due to magnetic collapse of FeO, dissolved in iron liquid in the outer core, and in solution in (Fe, Mg)O (magnesiowüstite) in the lowermost mantle[142]. Other compounds such as perovskites $(Mg,Fe)SiO_3$ [142] and $RFeO_3$ (R = Pr, Eu, Lu) [145, 146], or pyrite-like $(Mn,Fe)S_2$ and MnS_2 [147-151] also exhibit interesting spin-transitions under pressure.

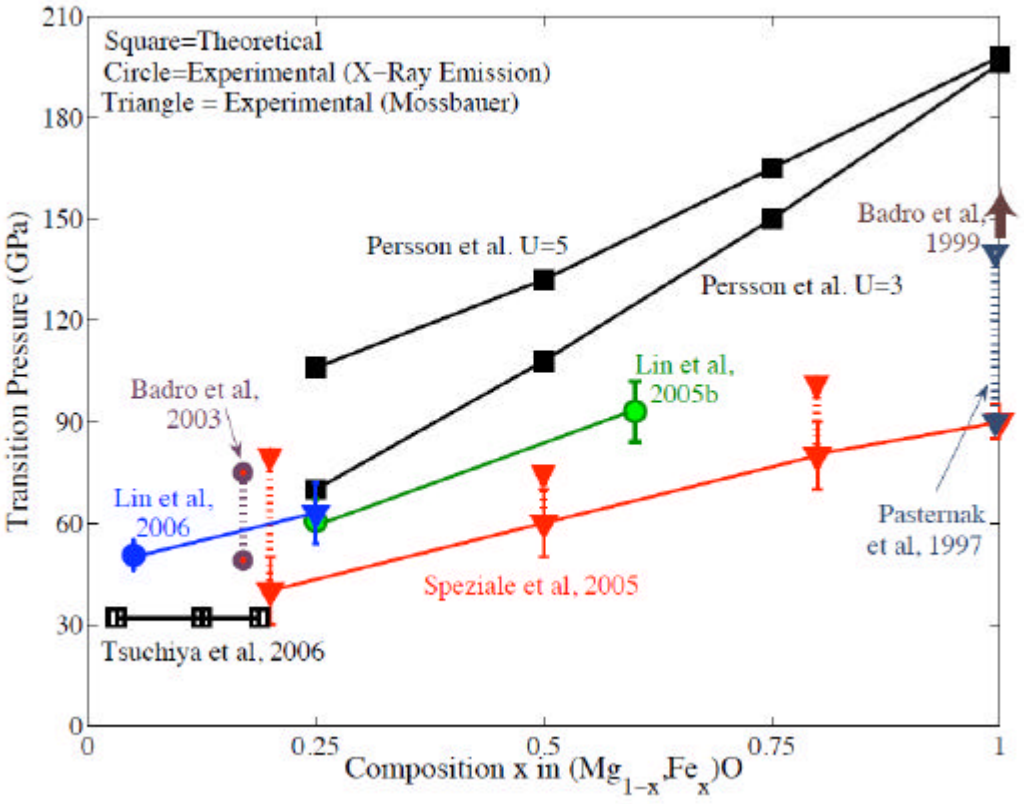

Fig. 14 *Calculated HS - LS spin transition pressures, in $(Mg_{1-x},Fe_x)O$, as a function of composition, compared with experiments. Adapted from [144].*

Rutile like-CrO_2 is a well-known ferromagnetic material with a Curie temperature of 392 K. The effect of pressure on the magnetic properties of CrO_2 has been investigated [152, 153] and pressure plays an important role in the stabilization of CrO_2, a material that is not found in nature. At ambient conditions Cr(IV) is not stable, but it can be stabilized under high pressure conditions [154-156]. Although nowadays a variety of synthetic routes for synthesising CrO_2 are known, acicular chromium dioxide was first synthesized by decomposing chromium trioxide in the presence of water at a temperature of 760 K and a pressure of 0.2GPa [157].

6 Conclusions

The information given in the preceding pages illustrates the fascination of transformations exhibited by condensed matter under high pressure conditions. Pressure can be utilized to change the atomic structure and chemical bonding of solids which in turn induces changes in the properties. The high pressure methods and technology developed in the last 50 years has been used successfully in a broad range of scientific disciplines, such as material science, solid state chemistry, physics, and Earth and planetary science. It is apparent that the field discussed here provides attractive prospects for future advances on a variety of aspects including the study of the physico-chemical properties of materials in extreme conditions, stabilization of new materials to help the understanding of the solid state, and to lead to functional properties for industrial applications.

7 References

[1] F. P. Bundy, J. Geophys. Res 85 (B12), 6930-6936 (1980)
[2] F. D. Murnaghan, Proceedings of the National Academy of Sciences 30, 244-247 (1944)
[3] F. Birch, Physical Review B 71, 809-824 (1947)
[4] L. D. Landau, Phys. Z. Sowjetunion 11, 26-47 (1937)
[5] P. Ehrenfest, Supplement Nr 75b zu den Mitteilungen aus dem Kamerlingh Onnes-Institut Leiden (1933)
[6] M. Ekman, B. Sadigh, K. Einarsdotter and P. Blaha, Physical Review B 58, 5296 (1998)
[7] W. Petry, Phase Transitions 31 (1-4), 119-136 (1991)
[8] R. Boehler, Hyperfine Interactions 128, 307-321 (2000)
[9] D. J. Dunstan, Recent developments in diamond anvil cells. In *High pressure chemistry, biochemistry and materials science*, R. Winter, and J. Jonas, Eds. Dordrecht / Boston / London, 1992.
[10] T. Hiroki, Review of High Pressure Science and Technology 11, 195-202 (2001)
[11] J. F. Lin, M. Santoro, V. V. Struzhkin, H. K. Mao, J. Shu and R. J. Hemley, Review of scientific instruments 75, 3302-3306 (2004)
[12] J. F. Lin, W. Sturhahn, J. Zhao, G. Shen and H. K. Mao, Geophysical Research Letters 31, L14611 (2004)
[13] W. J. Nellis, L. Seaman and R. A. Graham, *Shock waves in condensed matter*. AIP conference proceedings: New York, 1981; Vol. 78.
[14] M. L. Cohen, Journal de Physique 45, 7-11 (1984)
[15] A. Mujica, A. Rubio, A. Muñoz and R. J. Needs, Review of Modern Physics 75, 863-912 (2003)
[16] D. G. Pettifor, *Materials Science and Technology*. VCH: Weinheim, 1993; Vol. I.
[17] H. Katzke and P. Toledano, J. Phys.: Condens. Matter 19, 275204/1-10 (2007)
[18] J. M. Leger and J. Haines, European Journal of Solid State and Inorganic Chemistry 34 (7-8), 785-796 (1997)
[19] A. L. Ruoff, *Materials Science and Technology*. VCH: Weinheim, 1991; Vol. 5.
[20] W. B. Holzapfel, Reports on Progress in Physics 59, 29-90 (1996)
[21] R.J. Needs and A. Mujica, Physical Review B 51, 9652-9660 (1995)
[22] F. P. Bundy, W. A. Bassett, M. S. Weathers, R. J. Hemley, H. K. Mao and A. F. Goncharov, Carbon 34, 141-153 (1996)
[23] V. L. Sliwko, P. Mohn, K. Schwarz and P. Blaha, J Phys.: Condens Matter 8, 799-815 (1996)
[24] J. Cai and N. Chen, J Phys.: Condens Matter 19, 266207/1-12 (2007)
[25] J. Cai and N. Chen, Physical Review B 75 (13), 134109/1-12 (2007)
[26] V. Ozolins and A. Zunger, Physical Review Letters 82, 767-770 (1999)
[27] K. Kim, V. Ozolins and A. Zunger, Physical Review B 60 (12), R8449-R8452 (1999)
[28] M. Ekman, K. Persson and G. Grimvall, Physical Review B 62 (22), 14784-14789 (2000)
[29] J. R. Chelikowsky, Physical Review B 34 (8), 5295-5304 (1986)
[30] J. Haines and J. M. Leger, Physical Review B 55 (17), 11144-11154 (1997)
[31] A. Vegas and M. Jansen, Acta Crystallographica Section B 58, 38-51 (2002)
[32] G. Demazeau, Zeitschrift Fur Naturforschung Section B 61 (7), 799-807 (2006)
[33] G. Demazeau, H. Huppertz, J. A. Alonso, R. Pottgen, E. Moran and J. P. Attfield, Zeitschrift Fur Naturforschung Section B 61 (12), 1457-1470 (2006)
[34] F. Kanamaru, H. Miyamoto, Y. Mimura, M. Koizumi, M. Shimada, S. Kume and S. Shin, Materials Research Bulletin 5 (4), 257-& (1970)
[35] S. Kawasaki, M. Takano and Y. Takeda, Journal of Solid State Chemistry 121 (1), 174-180 (1996)
[36] G. Demazeau, B. Buffat, M. Pouchard and P. Hagenmuller, Journal of Solid State Chemistry 45 (1), 88-92 (1982)

[37] G. Demazeau, B. Buffat, M. Pouchard and P. Hagenmuller, Zeitschrift Fur Anorganische Und Allgemeine Chemie 491 (8), 60-66 (1982)
[38] J. Karpinski, E. Kaldis, E. Jilek, S. Rusiecki and B. Bucher, Nature 336 (6200), 660-662 (1988)
[39] J. M. Gallardo-Amores, N. Biskup, U. Amador, K. Persson, G. Ceder, E. Moran and M. E. Arroyo y de Dompablo, Chemistry of Materials 19(22), 5262-5271 (2007)
[40] M. E. Arroyo y de Dompablo, J. M. Gallardo-Amores, N. Biskup, E. Moran, H. Ehrenberg and U. Amador, Chemistry of Materials, Special Issue Energy Conversion 2010 (DOI: 10.1021/cm9018869) (2010)
[41] R. Bini, L. Ulivi, J. Kreutz and H. J. Jodl, Journal of Chemical Physics 112 (19), 8522-8529 (2000)
[42] M. I. Eremets, A. G. Gavriliuk, N. R. Serebryanaya, I. A. Trojan, D. A. Dzivenko, R. Boehler, H. K. Mao and R. J. Hemley, Journal of Chemical Physics 121 (22), 11296-11300 (2004)
[43] M. I. Eremets, A. G. Gavriliuk, I. A. Trojan, D. A. Dzivenko and R. Boehler, Nature Materials 3 (8), 558-563 (2004)
[44] C. Mailhiot, L. H. Yang and A. K. McMahan, Physical Review B 46 (22), 14419-14435 (1992)
[45] E. Wigner and H. B. Huntington, Journal of Chemical Physics 3 (12), 764-770 (1935)
[46] N. W. Ashcroft, Physical Review Letters 21 (26), 1748-1749 (1968)
[47] H. K. Mao and R. J. Hemley, Reviews of Modern Physics 66 (2), 671-692 (1994)
[48] W. J. Nellis, S. T. Weir and A. C. Mitchell, Shock Waves 9 (5), 301-305 (1999)
[49] C. Narayana, H. Luo, J. Orloff and A. L. Ruoff, Nature 393 (6680), 46-49 (1998)
[50] D. Eisenberg and W. Kauzmann, *The structure and properties of water*. Oxford University Press: London, 1969.
[51] C. Lobban, J. L. Finney and W. F. Kuhs, Nature 391 (6664), 268-270 (1998)
[52] V. F. Petrenko and R. W. Whitworth, *Physics of Ice*. Oxford University Press: Oxford, 1999.
[53] E. A. Zheligovskaya and G. G. Malenkov, Uspekhi Khimii 75 (1), 64-85 (2006)
[54] V. V. Struzhkin, A. F. Goncharov, R. J. Hemley and H. K. Mao, Physical Review Letters 78 (23), 4446-4449 (1997)
[55] A. F. Goncharov, V. V. Struzhkin, M. S. Somayazulu, R. J. Hemley and H. K. Mao, Science 273 (5272), 218-220 (1996)
[56] J. L. Aragones, M. M. Conde, E. G. Noya and C. Vega, Physical Chemistry-Chemical Physics 11 (3), 543-555 (2009)
[57] F. Liebau, *Structural chemistry of silicates*. Springer: Berlin / Heidelberg / New York, 1985.
[58] L. Finger and R. M. Hazen, *High-temperature and high-pressure crystal chemistry*. Mineralogical Society of America: 2000; Vol. 41.
[59] D. Santamaría-Pérez, A. Vegas and F. Liebau, Structure and Bonding 118, 121-177 (2005)
[60] R. Boehler and A. Chopelas, Geophysical Research Letters 18 (6), 1147-1150 (1991)
[61] T. Katsura, H. Yamada, T. Shinmei, A. Kubo, S. Ono, M. Kanzaki, A. Yoneda, M. J. Walter, E. Ito, S. Urakawa, K. Funakoshi and W. Utsumi In *Post-spinel transition in Mg2SiO4 determined by high P-T in situ X-ray diffractometry*, Workshop on Phase Transitions and Mantle Discontinuities, Potsdam, Germany, 2001, 2003; Elsevier Science Bv: Potsdam, Germany, 2003; pp 11-24.
[62] M. Murakami, K. Hirose, K. Kawamura, N. Sata and Y. Ohishi, Science 304, 855-858 (2004)
[63] A. R. Oganov and S. Ono, Nature 430, 445-448 (2004)
[64] H. Liander, Industrial Diamond Review (NOV), 412-415 (1980)
[65] F. P. Bundy, H. T. Hall, H. M. Strong and R. H. Wentorf, Nature 176 (4471), 51-55 (1955)
[66] F. P. Bundy, H. M. Strong, H. P. Bovenkerk and R. H. Wentorf, Journal of Chemical Physics 35 (2), 383-384 (1961)

[67] Q. Jiang, J. C. Li and G. Wilde, Journal of Physics-Condensed Matter 12 (26), 5623-5627 (2000)
[68] E. Y. Tonkov and E. G. Poniatovsky, *Phase transformations of elements under high pressure*. CRC Press: Boca Raton, FL, 2005.
[69] D. A. Young, *Phase diagrams of the elements*. University of California Press: Berkeley/ Los Angeles / Oxford, 1991.
[70] R. L. Smith and G. E. Sandland, Proceedings of the Institution of Mechanical Engineers I 623-641 (1922)
[71] J. Haines, J. M. Leger and G. Bocquillon, Annual Review of Materials Research 31 1-23 (2001)
[72] F. M. Gao, J. L. He, E. D. Wu, S. M. Liu, D. L. Yu, D. C. Li, S. Y. Zhang and Y. J. Tian, Physical Review Letters 91 (1), 015502/1-4 (2003)
[73] V. L. Solozhenko, D. Andrault, G. Fiquet, M. Mezouar and D. C. Rubie, Applied Physics Letters 78 (10), 1385-1387 (2001)
[74] Y. Zhang, H. Sun and C. F. Chen, Physical Review Letters 93 (19), 195504/1-4 (2004)
[75] V. L. Solozhenko, O. O. Kurakevych, D. Andrault, Y. Le Godec and M. Mezouar, Physical Review Letters 102 (1), 015506 (2009)
[76] F. R. Corrigan and F. P. Bundy, Journal of Chemical Physics 63 (9), 3812-3820 (1975)
[77] V. F. Britun, A. V. Kurdyumov and I. A. Petrusha, Materials Letters 41 (2), 83-88 (1999)
[78] V. L. Solozhenko, V. Z. Turkevich and W. B. Holzapfel, Journal of Physical Chemistry B 103 (15), 2903-2905 (1999)
[79] N. Dubrovinskaia, V. L. Solozhenko, N. Miyajima, V. Dmitriev, O. O. Kurakevych and L. Dubrovinsky, Applied Physics Letters 90 (10), 101912/1-3 (2007)
[80] D. Rafaja, V. Klemm, M. Motylenko, M. R. Schwarz, T. Barsukova, E. Kroke, D. Frost, L. Dubrovinsky and N. Dubrovinskaia, Journal of Materials Research 23 (4), 981-993 (2008)
[81] F. M. Gao, Physical Review B 73 (13), 132104/1-4 (2006)
[82] V. Blank, M. Popov, G. Pivovarov, N. Lvova, K. Gogolinsky and V. Reshetov In *Ultrahard and superhard phases of fullerite C-60: comparison with diamond on hardness and wear*, 8th European Conference on Diamond, Diamond-like and Related Materials/4th International Conference on the Applications of Diamond Films and Related Materials, Edinburgh, Scotland, Aug 03-08, 1997; Edinburgh, Scotland, 1997; pp 427-431.
[83] V. D. Blank, S. G. Buga, N. R. Serebryanaya, V. N. Denisov, G. A. Dubitsky, A. N. Ivlev, B. N. Mavrin and M. Y. Popov, Physics Letters A 205 (2-3), 208-216 (1995)
[84] E. Y. Tonkov, *High Pressure Phase Transformations Handbook 3* Overseas Publishers Association Amsterdam: Luxembourg, 1996.
[85] Q. Williams, R. J. Hemley, M. B. Kruger and R. Jeanloz, Journal of Geophysical Research-Solid Earth 98 (B12), 22157-22170 (1993)
[86] N. R. Keskar and J. R. Chelikowsky, Physical Review B 46 (1), 1-13 (1992)
[87] J. Badro, J. P. Itie and A. Polian, European Physical Journal B 1 (3), 265-268 (1998)
[88] P. Krempl, G. Schleinzer and W. Wallnofer In *Gallium phosphate, GaPO4: a new piezoelectric crystal material for high-temperature sensorics*, EUROSENSORS X Meeting, Louvain, Belgium, Sep 08-11, 1996; Louvain, Belgium, 1996; pp 361-363.
[89] J. L. Robeson, R. R. Winters and W. S. Hammack, Physical Review Letters 73 (12), 1644-1647 (1994)
[90] H. Sowa, Zeitschrift Fur Kristallographie 209 (12), 954-960 (1994)
[91] S. L. Chaplot and S. K. Sikka, Physical Review B 47 (10), 5710-5714 (1993)
[92] A. Jayaraman, D. L. Wood and R. G. Maines, Physical Review B 35 (16), 8316-8321 (1987)
[93] K. J. Kingma, R. J. Hemley, H. K. Mao and D. R. Veblen, Physical Review Letters 70 (25), 3927-3930 (1993)
[94] R. M. Wentzcovitch, C. da Silva, J. R. Chelikowsky and N. Binggeli, Physical Review Letters 80 (10), 2149-2152 (1998)

[95] M. E. Arroyo y de Dompablo and E. Moran, Zeitschrift Fur Naturforschung Section B 63 (6), 668-672 (2008)
[96] J. Pellicer-Porres, A. M. Saitta, A. Polian, J. P. Itie and M. Hanfland, Nature Materials 6 (9), 698-702 (2007)
[97] K. Gesi, Journal of the Physical Society of Japan 52 (10), 3322-3324 (1983)
[98] A. V. Kityk, V. P. Soprunyuk and O. G. Vlokh, Journal of Physics-Condensed Matter 5 (2), 235-246 (1993)
[99] H. Shimizu, N. Abe, N. Kokubo, N. Yasuda, S. Fujimoto, T. Yamaguchi and S. Sawada, Solid State Communications 34 (5), 363-368 (1980)
[100] R. E. Cohen, Nature 358 (6382), 136-138 (1992)
[101] G. A. Samara, Physical Review 151 (2), 378-379 (1966)
[102] G. A. Samara, Ferroelectrics 2 (4), 277-278 (1971)
[103] T. Ishidate, S. Abe, H. Takahashi and N. Mori, Physical Review Letters 78 (12), 2397-2400 (1997)
[104] M. I. McMahon and R. J. Nelmes, Chemical Society Reviews 35 943–963 (2006)
[105] R. Boehler, D. Santamaria-Perez, D. Errandonea and M. Mezouar, Journal of Physics: Conference Series 022018 (022010 pp.)-022018 (022010 pp.) (2008)
[106] R. Boehler, N. Vonbargen and A. Chopelas, Journal of Geophysical Research-Solid Earth and Planets 95 (B13), 21731-21736 (1990)
[107] G. Shen, H. K. Mao, R. J. Hemley, T. S. Duffy and M. L. Rivers, Geophysical Research Letters 25 (3), 373-376 (1998)
[108] D. Andrault, G. Fiquet, M. Kunz, F. Visocekas and D. Hausermann, Science 278 (5339), 831-834 (1997)
[109] L. S. Dubrovinsky, S. K. Saxena and P. Lazor In *Stability of beta-iron: A new synchrotron X-ray study of heated iron at high pressure*, EMU School on Modular Aspects of Minerals, Budapest, Hungary, Dec, 1997; E Schweizerbart'sche Verlags: Budapest, Hungary, 1997; pp 43-47.
[110] L. Dubrovinsky, N. Dubrovinskaia, O. Narygina, I. Kantor, A. Kuznetzov, V. B. Prakapenka, L. Vitos, B. Johansson, A. S. Mikhaylushkin, S. I. Simak and I. A. Abrikosov, Science 316 (5833), 1880-1883 (2007)
[111] Y. M. Ma, M. Eremets, A. R. Oganov, Y. Xie, I. Trojan, S. Medvedev, A. O. Lyakhov, M. Valle and V. Prakapenka, Nature 458 (7235), 182-U183 (2009)
[112] E. Gregoryanz, O. Degtyareva, M. Somayazulu, R. J. Hemley and M. Ho-kwang, Physical Review Letters 94 (18), 185502/1-4 (2005)
[113] J. G. Bednorz and K. A. Muller, Zeitschrift Fur Physik B-Condensed Matter 64 (2), 189-193 (1986)
[114] Z. Hiroi, M. Takano, M. Azuma and Y. Takeda, Nature 364 (6435), 315-317 (1993)
[115] C. N. R. Rao, R. Nagarajan and R. Vijayaraghavan, Superconductor Science & Technology 6 (1), 1-22 (1993)
[116] M. Hirabayashi, K. Tokiwa, H. Ozawa, Y. Noguchi, M. Tokumoto and H. Ihara, Physica C 219 (1-2), 6-8 (1994)
[117] H. Yamauchi, M. Karppinen and S. Tanaka In *Homologous series of layered cuprates*, International Symposium on Frontiers of High -T(c) Superconductivity, Morioka, Japan, Oct 27-29, 1995; Morioka, Japan, 1995; pp 146-150.
[118] E. Takayama-Muromachi, Chemistry of Materials 10 (10), 2686-2698 (1998)
[119] L. Gao, Y. Y. Xue, F. Chen, Q. Xiong, R. L. Meng, D. Ramirez, C. W. Chu, J. H. Eggert and H. K. Mao, Physical Review B 50 (6), 4260-4263 (1994)
[120] T. Cuk, V. V. Struzhkin, T. P. Devereaux, A. F. Goncharov, C. A. Kendziora, H. Eisaki, H. K. Mao and Z. X. Shen, Physical Review Letters 100 (21), 217003/1-4 (2008)
[121] P. L. Alireza, Y. T. C. Ko, J. Gillett, C. M. Petrone, J. M. Cole, G. G. Lonzarich and S. E. Sebastian, Journal of Physics-Condensed Matter 21 (1), 01220871-4 (2009)
[122] Y. Qiu, Wei Bao, Q. Huang, T. Yildirim, J. M. Simmons, M. A. Green, J. W. Lynn, Y. C. Gasparovic, J. Li, T. Wu, G. Wu, and X. H. Chen, Physical Review Letters 101 (25), 25700271-4 (2008)

[123] M. Rotter, M. Tegel and D. Johrendt, Physical Review Letters 101 (10), 107006/1-4 (2008)
[124] J. J. Hamlin, R. E. Baumbach, D. A. Zocco, T. A. Sayles and M. B. Maple, Journal of Physics-Condensed Matter 20 (36), 365220/1-6 (2008)
[125] T. M. McQueen, M. Regulacio, A. J. Williams, Q. Huang, J. W. Lynn, Y. S. Hor, D. V. West, M. A. Green and R. J. Cava, Physical Review B 78 (2), 024521/1-7 (2008)
[126] V. Vildosola, L. Pourovskii, R. Arita, S. Biermann and A. Georges, Physical Review B 78 (6), 064518 /1-10 (2008)
[127] H. Takahashi, K. Igawa, K. Arii, Y. Kamihara, M. Hirano and H. Hosono, Nature 453 (7193), 376-378 (2008)
[128] Y. Kamihara, H. Hiramatsu, M. Hirano, R. Kawamura, H. Yanagi, T. Kamiya and H. Hosono, Journal of the American Chemical Society 128 (31), 10012-10013 (2006)
[129] Y. Kamihara, T. Watanabe, M. Hirano and H. Hosono, Journal of the American Chemical Society 130 (11), 3296-3297 (2008)
[130] S. A. J. Kimber, A. Kreyssig, Y.-Z. Zhang, H. O. Jeschke, R. Valentí, F. Yokaichiya, E. Colombier, J. Yan, T. C. Hansen, T. Chatterji, R. J. McQueeney, P. C. Canfield, A. I. Goldman and D. N. Argyriou, Nature Materials 8, 471-475 (2009)
[131] J. Caulfield, W. Lubczynski, F. L. Pratt, J. Singleton, D. Y. K. Ko, W. Hayes, M. Kurmoo and P. Day, Journal of Physics-Condensed Matter 6 (15), 2911-2924 (1994)
[132] R. L. Greene and E. M. Engler, Physical Review Letters 45 (19), 1587-1590 (1980)
[133] M. Itaya, Y. Eto, A. Kawamoto and H. Taniguchi, Physical Review Letters 102 (22), 22700371-4 (2009)
[134] H. Taniguchi, M. Miyashita, K. Uchiyama, R. Sato, Y. Ishii, K. Satoh, N. Mori, M. Hedo and Y. Uwatoko, Journal of the Physical Society of Japan 74 (5), 1370-1373 (2005)
[135] H. Taniguchi, M. Miyashita, K. Uchiyama, K. Satoh, N. Mori, H. Okamoto, K. Miyagawa, K. Kanoda, M. Hedo and Y. Uwatoko, Journal of the Physical Society of Japan 72 (3), 468-471 (2003)
[136] H. Taniguchi, M. Miyashita, K. Uchiyama, K. Satoh, N. Mori, H. Okamoto, K. Miyagawa, K. Kanoda, M. Hedo and Y. Uwatoko In *Superconductivity induced by extremely high pressure in layered organics, beta '-(BEDT-TTF)(2)ICI2*, 5th International Symposium on Crystalline Organic Metals, Superconductors and Ferromagnets (ISCOM2003), Port Bourgenay, FRANCE, Sep 21-26, 2003; Port Bourgenay, FRANCE, 2003; pp 273-276.
[137] E. Babaev, A. Sudbo and N. W. Ashcroft, Nature 431 (7009), 666-668 (2004)
[138] E. Babaev, A. Sudbo and N. W. Ashcroft, Physical Review Letters 95 (10), 10530171-4 (2005)
[139] T. Yagi, T. Suzuki and S. Akimoto, Journal of Geophysical Research-Solid Earth and Planets 90 (NB10), 8784-8788 (1985)
[140] H. K. Mao, J. F. Shu, Y. W. Fei, J. Z. Hu and R. J. Hemley In *The wustite enigma*, A E Ringwood Memorial Symposium on High Pressure Mineral Physics and Petrochemistry, in Memory of Professor Ted Ringwood, Hiroshima, Japan, Nov 14-16, 1994; Hiroshima, Japan, 1994; pp 135-145.
[141] J. Badro, V. V. Struzhkin, J. F. Shu, R. J. Hemley, H. K. Mao, C. C. Kao, J. P. Rueff and G. Y. Shen, Physical Review Letters 83 (20), 4101-4104 (1999)
[142] R. E. Cohen, Mazin, II and D. G. Isaak, Science 275 (5300), 654-657 (1997)
[143] S. A. Gramsch, R. E. Cohen and S. Y. Savrasov, American Mineralogist 88 (2-3), 257-261 (2003)
[144] K. Persson, A. Bengtson, G. Ceder and D. Morgan, Geophysical Research Letters 33 (16), L16306/1-5 (2006)
[145] G. K. Rozenberg, M. P. Pasternak, W. M. Xu, L. S. Dubrovinsky, S. Carlson and R. D. Taylor, Europhysics Letters 71 (2), 228-234 (2005)
[146] W. M. Xu, O. Naaman, G. H. Rozenberg, M. P. Pasternak and R. D. Taylor, Physical Review B 64 (9), 094411/1-9 (2001)
[147] K. Persson, G. Ceder and D. Morgan, Physical Review B 73 (11), 115201/1-8 (2006)

[148] T. Chattopadhyay and H. G. Vonschnering, Journal of Physics and Chemistry of Solids 46 (1), 113-116 (1985)
[149] D. Hobbs and J. Hafner, Journal of Physics-Condensed Matter 11 (42), 8197-8222 (1999)
[150] T. A. Bither, R. J. Bouchard, W. H. Cloud, P. C. Donohue and W. J. Siemons, Inorganic Chemistry 7 (11), 2208-2220 (1968)
[151] T. A. Bither, C. T. Prewitt, J. L. Gillson, Biersted.Pe, R. B. Flippen and H. S. Young, Solid State Communications 4 (10), 533-535 (1966)
[152] S. F. Matar and G. Demazeau, Chemical Physics Letters 407 (4-6), 516-521 (2005)
[153] V. A. Sidorov, A. V. Rakhmanina and O. A. Morya, Solid State Communications 139 (7), 360-362 (2006)
[154] R. C. Devries, Materials Research Bulletin 2 (11), 999-& (1967)
[155] P. Porta, J. P. Remeika, M. Marezio and P. D. Dernier, Materials Research Bulletin 7 (2), 157-161(1972)
[156] W. B. White and R. Roy, Geochimica Et Cosmochimica Acta 39 (6-7), 803-817 (1975)
[157] T. J. Swoboda, N. L. Cox, M. S. Sadler, A. L. Oppegard, J. N. Ingraham and P. Arthur, Journal of Applied Physics 32 (3), S374-S375 (1961)